Preparation of Nanohybrid Solid-State Electrolytes with Liquidlike Mobilities by Solidifying Ionic Liquids with Silica Particles

Satoshi Shimano, Haoshen Zhou, and Itaru Honma*

Energy Technology Research Institute, National Institute of Advanced Industrial Science and Technology (AIST), 1-1-1 Umezono, Tsukuba, Ibaraki 305-8568, Japan

The novel ion-conducting properties of nanohybrid materials consisting of ionic liquids and nanosized silica were investigated. The nanohybrid materials can be prepared by a simple mechanical milling process, and their compositions can be controlled over a wide range of ratios of ionic liquid to nanosized silica particles. Interestingly, the hybrid materials remain in the solid state even when as much as 90 wt % of the ionic liquid is incorporated in the matrix, provided that nanosized silica with a particle size of 7 nm is used. The hybrid materials exhibit large conductivities from room temperature to the intermediate temperature region. For example, the conductivity of a [BMIm][TFSI]/silica (7 nm) hybrid containing 60 wt % ionic liquid increased to 1×10^{-2} S cm^{-1} at 300 °C, although the solid hybrids were stable even at the intermediate temperatures. The nanosize confinement of liquid molecules within the silica particles is presumed to be responsible for the liquidlike conductivities in the solid phase and for the stability of the ionic liquids to fluidity and evaporation. Nanosize effects of the ionic liquid on the conducting properties were also demonstrated.

1. Introduction

The properties of the electrolytes are crucial to the performance of electrochemical devices such as fuel cells, lithium-ion rechargeable batteries, and electric double-layer capacitors. The ranges of operating conditions, such as the temperature or the electrochemical potential, for such devices are limited by the stability of the electrolyte. There are high and growing demands for the improvement of the performance of electrochemical devices, such as increased power, increased energy density, better reliability, and cycleability over a long period. For these purposes, the development of novel electrolytes with a high conductivity for the object ions (protons for fuel cells, lithium ions for lithium batteries), a high thermal stability, a minimal resistance to the electrode materials, and the ability to be mechanically self-supporting are attracting increasing amounts of attention.

Ionic liquids, which are composed entirely of cations and anions, are a new class of novel electrolyte with a high conductivity for ions, a wide electrochemical window, and a good thermal stability; they are also nonvolatile and flame-resistant. Increasingly, investigators are paying attention to the application of these liquids in various electrochemical devices, such as fuel cells,[1−4] lithium-ion rechargeable batteries,[5−7] electric double-layer capacitors,[8,9] dye-sensitized photoelectrochemical cells,[10−19] and electrochemical actuators.[20]

Attempts have been made to solidify the ionic liquids into mechanically self-supporting solid-state electrolytes by five different methods: (i) impregnation into an organic polymer,[21−24] (ii) copolymerization with an ionic-liquid monomer,[25−33] (iii) solidification using low-molecular-weight gelating agents,[12,13,34] (iv) confinement within inorganic gels,[35−37] and (v) gelation with nanoparticles.[15−19]

(5) Fung, Y. S.; Zhou, R Q. *J. Power Sources* **1999,** *81−82,* 891−895.
(6) Tiyapiboonchaiya, C.; Pringle, J. M.; Sum, J.; Byrne, N.; Howlett, P. C.; MacFarlane, D. R.; Forsyth, M. *Nat. Mater.* **2004,** *3,* 29−32.
(7) Sakaebe, H.; Matsumoto, H.; Tatsumi, K. *J. Power Sources* **2005,** *146,* 693−697.
(8) Ue, M.; Takeda, M.; Takehara, M.; Mori, S. *J. Electrochem. Soc.* **1997,** *144,* 2684−2688.
(9) Ue, M.; Takeda, M.; Toriumi, A.; Kominato, A.; Hagiwara, R.; Ito, Y. *J. Electrochem. Soc.* **150,** *4,* A499−A502.
(10) Matsumoto, M.; Wada, Y.; Kitamura, T.; Shigaki, K.; Inoue, T.; Ikeda, M.; Yanagida, S. *Bull. Chem. Soc. Jpn.* **2001,** *74,* 387−393.
(11) Sakaguchi, S.; Ueki, H.; Kato, T.; Kadoa, T.; Shiratuchi, R.; Takashima, W.; Kaneto, K.; Hayase, S. *J. Photochem. Photobiol.,* A **2004,** *164,* 117−122.
(12) Kubo, W.; Murakoshi, K.; Kitamura, T.; Wada, Y.; Hanabusa, K.; Shirai, H.; Yanagida, S. *Chem. Lett.* **1998,** 1241−1242.
(13) Kubo, W.; Kambe, S.; Nakade, S.; Kitamura, T.; Hanabusa, K.; Wada, Y.; Yanagida, S. *J. Phys. Chem. B* **2003,** *107,* 4374−4381.
(14) Kato, T.; Okazaki, A.; Hayase, S. *Chem. Commun.* **2005,** 363−365.
(15) Stathatos, E.; Lianos, P.; Zakeeruddin, S M.; Liska, P.; Gratzel, M. *Chem. Mater.* **2003,** *15,* 1825−1829.
(16) Wang, P.; Zakeeruddin, S. M.; Comte, P.; Exnar, I.; Gratzel. M. *J. Am. Chem. Soc.* **2003,** *125,* 1166−1167.
(17) Wang, P.; Zakeeruddin, S. M.; Exnarb, I.; Gratzel, M. *Chem. Commun.* **2002,** 2972−2973.
(18) Wang, P.; Zakeeruddin, S. M.; Gratzel. M. *J. Fluorine Chem.* **2004,** *125,* 1241−1245.
(19) Usui, H.; Matsui, H.; Tanabe, N.; Yanagida, S. *J. Photochem. Photobiol.,* A **2004,** *164,* 97−101.
(20) Ding, J.; Zhou, D.; Spinks, G.; Wallace, G.; Forsyth, S.; Forsyth, M.; MacFarlane D. *Chem. Mater.* **2003,** *15,* 2392−2398.
(21) Fuller, J.; Breda, A. C.; Carlin, R. T. *J. Electrochem. Soc.* **1997,** *144,* L67−L69.
(22) Fuller, J.; Breda, A. C.; Carlin, R. T. *J. Electrochem. Soc.* **1998,** *459,* 29−34.
(23) Noda, A.; Watanabe, M. *Electrochim. Acta* **2000,** *45,* 1265−1270.
(24) Susan, A. H.; Kaneko, T.; Noda, A.; Watanabe, M. *J. Am. Chem. Soc.* **2005,** *127,* 4976−4983.

* Corresponding author. E-mail: i.homma@aist.go.jp. Tel: 81-29-861-5648. Fax: 81-29-861-5799.
(1) Noda, A.; Susan, M. A. B. H.; Kudo, K.; Mitsushima, S.; Hayamizu, K.; Watanabe, M. *J. Phys. Chem. B* **2003,** *107,* 4024−4033.
(2) de Souza, R. F.; Padilha, J. C.; Goncalves, R. S.; Dupont, J. *Electrochem. Commun.* **2003,** *5,* 728−731.
(3) Hagiwara, R.; Nohira, T.; Matsumoto, K.; Tamba, Y. *Electrochem. Solid-State Lett.* **2005,** *8,* A231−A233.
(4) Kudo, K.; Mitsushima, S.; Kamiya, N.; Ota, K. *Electrochemistry* **2005,** *73,* 272−274.

We adopted the last of these strategies: gelation of an ionic liquid with nanoparticles. There are several reports regarding the solidification of ionic liquid with nanoparticles such as silica,[16−18] titania,[19] and carbon nanotubes.[19] Wang et al.[16−18] prepared quasi-solid-state electrolytes by adding fumed silica to ionic liquids and used the products to enhance the thermal stability of dye-sensitized solar cells. Usui et al.[19] explored the properties of dye-sensitized solar cells prepared using an ionic liquid electrolyte dispersed in carbon nanotubes or titania nanoparticles. There have been, however, no adequate studies on the high-temperature tolerance or the conduction mechanism of such hybrid electrolytes.

We attempted to synthesize solid-state electrolytes by solidifying ionic liquids with inorganic nanoparticles, and we explored their conducting properties in the intermediate temperature range from room temperature to 300 °C; we also examined the morphology of the gel structure and we identified some novel nanoscale effects on the conducting properties of the hybrid electrolytes. We focused particular attention on a nanoscale effect on the conducting properties of the ionic liquids. In terms of their stabilities at intermediate temperatures, the hybrid materials that were synthesized exhibited a relatively large ionic conductivity up to 300°C as a result of the stabilization of the ionic liquid molecules at the interfaces of nanosized silica; the materials could, therefore, form a new category of solid-state electrolytes with a liquidlike conductivity over a wide range of temperatures. The molecular confinement effect of ionic liquid at the interfaces of nanosized silica with a high surface area is, presumably, responsible for the stability of the hybrid electrolyte at high temperatures without a significant reduction in the liquidlike ion mobility.

2. Experimental Section

2.1. Materials. 1-Butyl-3-methylimidazolium bis(trifluoromethanesulfonyl)imide ([BMIm][TFSI]) was purchased from Kanto Chemical Corporation. [Im]$_4$[HTFSI] was synthesized from imidazole (Im) (Tokyo Kase Kogyo Co.) and bis(trifluoromethanesulfonyl)amide (HTFSI) (Wako Pure Chemical Industries Co.) in a 1:4 mole ratio; the components were mixed slowly to prevent an increase in the temperature as a result of the reaction. [EtIm]$_4$[HTFSI] was similarly
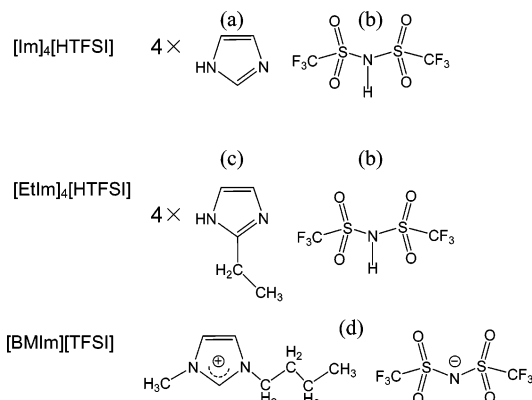

Figure 1. Molecular structures of the components of ionic liquids: (a) imidazole (Im), (b) bis(trifluoromethanesulfonyl)amide (HTFSI), (c) 2-ethylimidazole (EtIm), and (d) 1-butyl-3-methylimidazole bis(trifluoromethanesulfonyl)azanide (TFSI).

prepared from 2-ethylimidazole and HTFSI. In all cases, the ionic liquids were synthesized and handled in an argon-filled glove box. The chemical structures of the ionic liquids are shown in Figure 1. The measured densities of the ionic liquids were 1.42 g cm^{-3} for [Im]$_4$[HTFSI], 1.26 g cm^{-3} for [EtIm]$_4$[HTFSI], and 1.47 g cm^{-3} for [BMIm][TFSI] at 25°C.

Four types of silica particle were used: fumed silica 7 nm (grain size 7 nm, surface area 390 ± 40 m^2 g^{-1}, Sigma Co.), fumed silica 14 nm (surface area 200 ± 25 m^2 g^{-1}, Sigma Co.), silicon dioxide 70 nm (Wako Pure Chemical Industries Co.), and silicon dioxide (reagent grade, Wako Pure Chemical Industries Co.). The density of silica is 2.2 g cm^{-3}. The various silica samples were heated for 10 h at 120 °C under a vacuum below 0.01 MPa before they were mixed with the ionic liquids.

2.2. Synthesis of Hybrid Materials by Ball-Milling. The ionic liquids and the silica were mixed by a planetary mill (Pulverisette 5, Fritsch Co.), using a pod (50 mL) and 10 balls (10 mm φ) made of zirconium oxide. The dried silica (about 0.5 mg) and the ionic liquid were mixed in the pod in an argon-filled glove box and then mechanically milled for 5 h at a rotation speed of 200 rpm.

2.3. Ion Conductivity Measurements. The ion conductivities of pellets of the hybrid materials were measured by the ac impedance method. Pellets of the hybrid materials with a diameter of 7 mm and a thickness of 1.5 mm were fabricated by pressing at 4 MPa with Teflon plate covers and then sandwiched between two parallel, 5 mm diameter, gold-coated electrodes. The ion conductivities of the samples were measured in a chamber under flowing nitrogen by the ac impedance method over the frequency range from 1 × 10^6 to 1 Hz by using a Solartron 1260 impedance analyzer.

2.4. Fuel-Cell Measurements. Membrane electrode assemblies (MEAs), 7 mm in diameter and 0.2 mm thick, comprising the hybrid electrolytes and gas-diffusion Pt/carbon electrodes (Pt loading 0.4 mg cm^{-3}, E-TEK, Inc.) were made simply by pressing at 4 MPa at 120°C for a few minutes. Dry oxygen and dry hydrogen (0.1 MPa) were used to test the operation of the fuel cell, and its $I-V$ characteristics under nonhumidification conditions were recorded.

3. Results

3.1. Morphology of the Hybrid Electrolytes. With all three ionic liquids, the hybrid electrolytes remained in the solid state when the volume fraction of the ionic liquid was between 10 and 90 wt %. A photograph of pellets of [BMIm]-[TFSI]/SiO$_2$ (7 nm), as an example, is shown in Figure 2a. The pure ionic liquid [BMIm][TFSI] is transparent and

(25) Yoshimoto, N.; Shirai, T.; Morita, M. *Electrochim. Acta* **2005**, *50*, 3866−3871.
(26) Yoshizawa, M.; Ogihara, W.; Ohno, H. *Polym. Adv. Technol.* **2002**, *13*, 589−594.
(27) Yoshizawa, M.; Ohno, H. *Electrochim. Acta* **2001**, *46*, 1723−1728.
(28) Ohno, H. *Electrochim. Acta* **2001**, *46*, 1407−1411.
(29) Ohno, H.; Ito, K. *Chem. Lett.* **1998**, *27*, 751−752.
(30) Ohno, H.; Yoshizawa, M.; Ogihara, W. *Electrochim. Acta* **2004**, *50*, 255−261.
(31) Hirao, M.; Ito-Akita, K.; Ohno, H. *Polym. Adv. Technol.* **2000**, *11*, 534−538.
(32) Hirao, M.; Ito, K.; Ohno, H. *Electrochim. Acta* **2000**, *45*, 1291−1294.
(33) Washiro, S.; Yoshizawa, M.; Nakajima, H.; Ohno, H. *Polymer* **2004**, *45*, 1577−1582.
(34) Ikeda, A.; Sonoda, K.; Ayabe, M.; Tamaru, S.; Nakashima, T.; Kimizuka, N.; Shinkai, S. *Chem. Lett.* **2001**, 1154−1155.
(35) Neouze, M. A.; Le Bideau, J.; Leroux, F.; Vioux, A. *Chem. Commun.* **2005**, 1082−1084.
(36) Shi, F.; Fang, Q.; Li, D.; Deng, Y. *Chem.−Eur. J* **2005**, *11*, 5279−5288.
(37) Shi, F.; Deng, Y. *Spectrochim. Acta, Part A* **2005**, *62*, 239−244.
(38) Archie, G. E. *Trans. Am. Inst. Mech. Eng.* **1942**, *146*, 54−61.
(39) Deki, S.; Mizuhata, M.; Nakamura, K.; Kajinami, A.; Kanaji, Y. *J. Electrochem. Soc.* **1992**, *139*, 1544−1548.
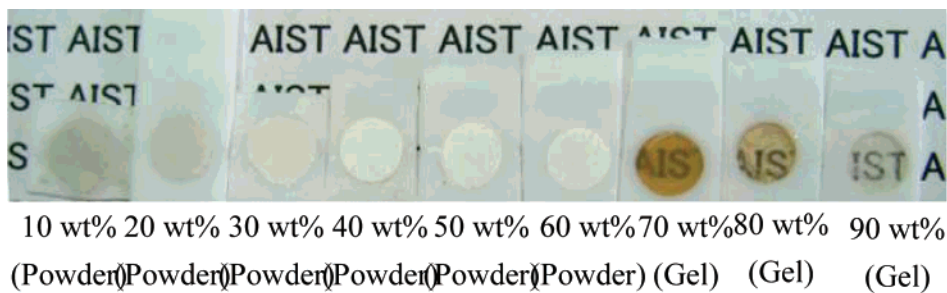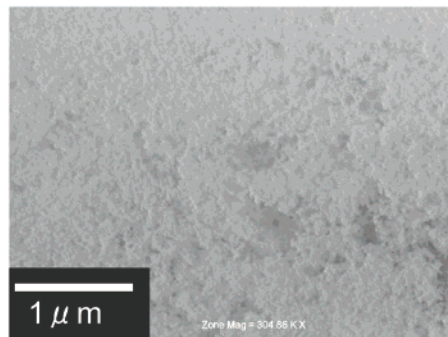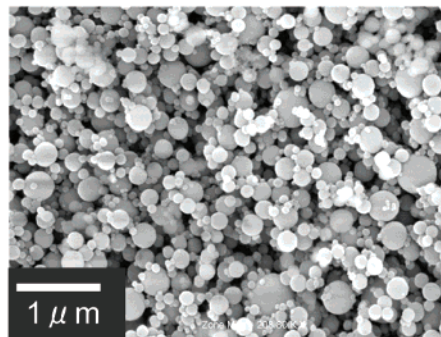
10 wt% 20 wt% 30 wt% 40 wt% 50 wt% 60 wt% 70 wt% 80 wt% 90 wt%
(Powder)(Powder)(Powder)(Powder)(Powder)(Powder) (Gel)   (Gel)   (Gel)

(a) [BMIm][TFSI]/SiO₂(7nm)

(b) [Im]₄[HTFSI]/SiO₂(7 nm)   (c) [Im]₄[HTFSI]/SiO₂(7 nm)
40 wt%–IL (Powder)   70 wt%–IL (Gel)

Figure 2. (a) Photograph of IL([BMIm][TFSI]/SiO₂ (7 nm) hybrid materials with various ionic liquid compositions from 10 to 90 wt % and SEM images of (b) powder state (40 wt % IL) and (c) gel state (70 wt % IL).

Table 1. Grain Sizes and Surface Areas of the Silica Samples

silica source	grain size (nm, unless noted)	surface area ($m^2 g^{-1}$)
silica particles	100 μm	0.01
silica particles	70	39
fumed silica	14	195
fumed silica	7	390

Table 2. Morphologies of the [BMIM][TFSI]/SiO₂ Hybrid Materials[a]

	IL conc. (wt %)								
	10	20	30	40	50	60	70	80	90
SiO₂ 100 μm	P	G	G	G	L	L	L	L	
SiO₂ 70 nm	P	P	G	G	G	VL	VL	VL	VL
SiO₂ 14 nm	P	P	P	P	P	G	G	G	G
SiO₂ 7 nm	P	P	P	P	P	P	G	G	G

[a] P, white powder; G, solid gel; VL, viscous liquid; L, liquid containing particles.

Figure 3. Ionic liquid composition dependence of the ion conductivity of the IL/SiO₂ (7 nm) hybrids at 25°C.

colorless. Pellets containing 70−90 wt % ionic liquid were semitransparent gels, whereas materials containing less than 60 wt % ionic liquid were entirely solid-state bulky materials. The apparent morphologies of [BMIm][TFSI]/SiO₂ hybrids with different silica sizes are listed in Table 2.

Interestingly, hybrids containing more than 90 wt % of ionic liquid are solid materials if silicas with a particle size of less than 14 nm are used as the solidifying agents: this phenomenon was observed for all three ionic liquids that we studied.

The scanning electron micrographs of the [BMIm][TFSI]/SiO₂ (7 nm) hybrid, before preparing the pellets, are shown in Figure 2 for ionic liquid concentrations of (b) 40 and (c) 70 wt %. In the former case, no dense body of solid particle aggregates was observed, and in the latter case, spherical liquidlike droplets with large diameters (50−300 nm) were observed. Starting hybrid materials containing higher con-
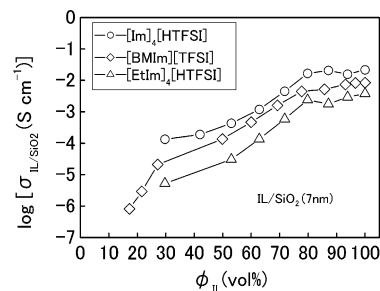
centrations of ionic liquid show surface morphologies associated with a liquidlike nature.

3.2. Spectroscopic Analysis of Hybrid Electrolytes. The infrared and Raman spectra of the hybrid materials were recorded. The spectra of the hybrid materials were found to be superpositions of those of the ionic liquids and silica.

No significant changes were observed in the individual spectra, suggesting that strong interactions, such as hydrogen bonds between the ionic liquids and the silica, are not prevalent in the hybrid materials.

3.3. The Ion Conductivity of the Hybrid Electrolytes. The ion conductivities of the hybrid materials of the three different ionic liquids at 25 °C were plotted as a function of their volume ratios of ionic liquids to silica, as shown in Figure 3. The volumetric concentrations of ionic liquid were calculated according to the densities of silica and the ionic liquids. In all the cases, the conductivity increased with the fraction of the ionic liquid up to 80 vol % and then remained almost constant above this fraction. The conductivity, which exceeds 1×10^{-3} S cm^{-1} at room temperature, is quite high for a solid-state electrolyte, and is larger than that of lithium-
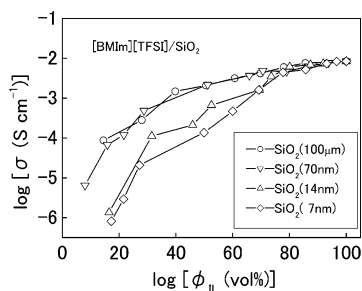
Nanohybrid Solid State Electrolytes with Liquidlike Mobilities

Chem. Mater., Vol. 19, No. 22, 2007 5219

Figure 4. Ion conductivity of the [BMIm][TFSI]/SiO$_2$ hybrids with various particle sizes of silica.

Figure 5. Temperature dependence of ion conductivity of the [BMIm]-[TFSI]/SiO$_2$ hybrid with different ionic liquid composition at 40, 60, and 80 wt %, respectively.

conducting solid polymer electrolytes used in various devices.[6] The ion conductivities of hybrid materials at 25°C as a function of the size of the silica are shown in Figure 4. The ion conductivities of the hybrid materials containing 70 nm silica are almost the same as those containing 100 μm silica; however, the ion conductivities of hybrids containing silica particles with a size of 14 as well as 7 nm exhibited quite different characteristics and were significantly dependent on the composition of the ionic liquids. The conductivities increased rapidly with increasing proportion of ionic liquid, particularly from 20 to 80 vol %, whereas the conductivities at the same ionic liquid composition are different; those are larger at the silica particle size of 70 nm and 100 μm.

3.4. Thermal Stability of Hybrid Electrolytes. The thermal stabilities of the hybrid materials were measured at 25−500 °C by thermogravimetry/differential thermal analysis (TGDTA2000S, Mac Science). In the case of the [Im]$_4$-[HTFSI] hybrids, which incorporate excess imidazole base to give a higher ion conductivity, some imidazole molecules from the [Im]$_4$[HTFSI] compounds are evaporated below 257 °C, and the [Im]$_4$[HTFSI] was converted into the stoichiometric [Im][HTFSI]. No significant changes, such as decomposition or evaporation of stoichiometric [Im][HTFSI] compounds, were observed below 300°C.

The decomposition of stoichiometric [BMIm][TFSI] began at around 350°C, which is almost the same as the decomposition temperature of the original ionic liquid. (see the Supporting Information, Figures S1−S4) Although the structural stability of the hybrid materials have been tentatively characterized by TG-DTA analysis, the obtained data suggest the stability of the hybrid electrolyte materials at intermediate temperatures. Kosmulski et al., reported the thermal stability of the ionic liquids and discussed problems of evaluating by the fast TG-DTA scans, where usually, the decomposition reaction and heat transfer in the liquids are too slow at low temperatures, so that the experimental data may lag behind the real decompositions. In the present investigations, the rapid screening of the thermal stability of the hybrid has been obtained by TG-DTA measurements.[40]

The ion conductivities of [BMIm][TFSI]/SiO$_2$ (7 nm) hybrids containing various concentrations of ionic liquids (40, 60, and 80 wt %) were measured over the temperature range 25−300°C under dry conditions (Figure 5). The hybrid materials containing 80 wt % ionic liquids became viscous at around 120°C, and the conductivity decreased above this
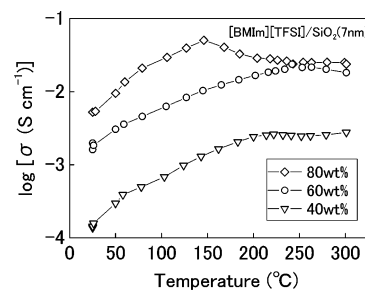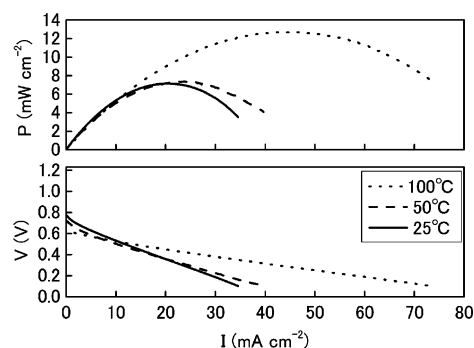

Figure 6. Dry H$_2$/O$_2$ cell performance with [Im]$_4$[HTFSI]/SiO$_2$ (7 nm) (IL 60 wt %) electrolyte. Cell voltage (V) and power density (P) are plotted against the current density (I).

temperature. However, hybrids containing 60 wt % ionic liquids showed a monotonic increase in conductivity over the temperatures scan and possessed large conductivities of more than 1×10^{-2} S cm^{-1} in the intermediate temperature region (200−300°C). These results show that hybrid electrolytes in which the ionic liquids are solidified by nanosized silica particles are fast-ion-conducting, solid-state electrolytes at intermediate temperature, and their conductivities are among the highest reported for solid-state materials.

3.5. Fuel-Cell Test under Nonhumidifying Conditions. The viability of using the hybrid materials as fuel-cell electrolytes under nonhumidifying conditions was tested. [Im]$_4$[HTFSI] was recently studied as a proton-conducting ionic liquid for fuel cells.[1] The performance of a fuel cell using [Im]$_4$[HTFSI]/SiO$_2$ (7 nm) hybrid (60 wt % ionic liquid content) as an electrolyte is shown in Figure 6. The open-circuit voltages were about 0.8 V at 25°C. The power density increased with temperature to a maximum of 12 mW cm^{-2} at 100°C. The power density at 150°C, however, decreased as a result of some evaporation of imidazole molecules from the hybrid electrolytes in the ionic liquids. These results indicate that the hybrid materials are proton-conducting materials that are suitable for fuel-cell operations.

4. Discussion

4.1. Concentration Dependence of the Ion Conductivity. Archie's law[38] provides an equation that relates the ion conductivity of a hybrid material to the volume ratio of the ion-conducting component.

$$\sigma_{\mathrm{IL/SiO_2}} = a\sigma_{\mathrm{IL}}\phi_{\mathrm{IL}}{}^{m} \qquad (1)$$

Here, $\sigma_{\mathrm{IL/SiO_2}}$ represents the ion conductivity of the hybrid

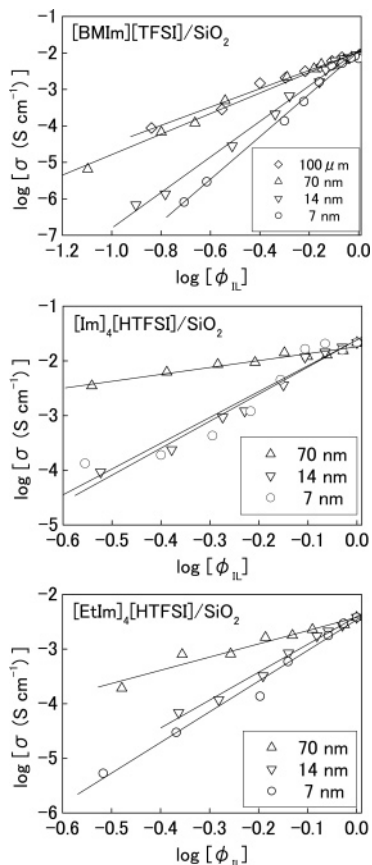(40) Kosmulski, M.; Gustafsson, J.; Rosenholm, J. B. *Thermochim. Acta* **2004**, *412*, 47.

Figure 7. Archie's plot (log σ – log φ_{IL}) for three different hybrid materials ([BMIm][TFSI], [Im]$_4$[HTFSI], and [EtIm]$_4$[TFSI]) with various silica particle sizes.
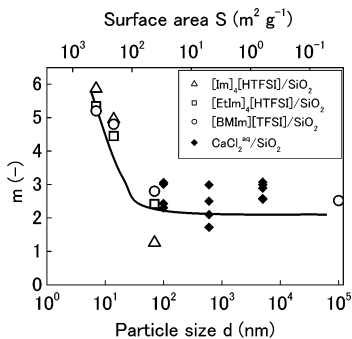

Figure 8. Shift in the value of "*m*" in the Archie's plots with respect to the silica particle size.

material and σ_{IL} that of the pure ionic liquid; ϕ_{IL} is the volume fraction of the ionic liquid and a is a proportionality factor. Figure 7 demonstrates that Archie's law can be applied to the conducting properties of our hybrid materials. The linearity of the Archie plot was confirmed for the three different ionic liquids. The value of *m* in eq 1, which corresponds to the slope of the plots in Figure 7, indicates the power dependence of the conductivity against the volumetric composition of the ionic liquids in the hybrid materials. Apparently, the value of *m* increased when small silica particles were used in the hybrids, especially for sizes smaller than 14 nm. The values of *m* are plotted as a function of the silica particle size in Figure 8. The values of *m* were about 2.5 when silica particle sizes were larger than 70 nm. These values agree with a value investigated for aqueous solutions: Deki and co-worker[39] reported that the value of

m for hybrid materials comprising aqueous solutions of calcium chloride and aluminum oxide is around 2.5. However, the hybrid materials with nanosized silica particles (diameter smaller than 14 nm) show a marked enhancement in *m*, as shown in Figure 8; the value increases to around 5–6 as the particle size decreases to 7 nm. These results indicate that there is a marked change in the ion-conducting mechanism with nanoscale media; i.e., a nanoscale effect on the liquid-phase conduction in the confined space has been demonstrated. A drastic change in the conducting properties of salt solutions in the solid insulating particles has been reported by A. J. Bhattacharyya et al.,[41,4241–42] where the presence of the second phase can increase the total ion conductivity of the "soggy sand electrolytes" because of the interfacial interactions. The chemical potential of mobile ions has been shifted under the space charge region from the interface, resulting in the nonequilibrium transport of the mobile species with an enhancement of carrier concentration and/or mobility.

Our comprehension of this phenomenon is that the ion-conduction path of the ionic liquids in the hybrid materials, particularly on a nanoscale, is quite different from that of bulky ionic liquids. The local structure of the ionic liquids at nanoscale interfaces may be modified by the confinement between nanosized silica particles, and this nanosize confinement of liquid molecules may mediate a mechanism of ionic transport that requires enhanced IL concentration dependence (value "*m*") to form a rapid conduction path. It is plausible that the ionic liquid on the interface are structured and solidified when strong interactions between the ionic liquids and the silica surfaces prevail; on the other hand, this interaction also results in thermal stability up to the 300°C.

5. Conclusion

Solid-state hybrid materials consisting of ionic liquids and silica nanoparticles were prepared. These hybrid materials showed stable ionic conductivities over a wide range of temperatures: the conductivity was 1×10^{-2} S cm^{-1} at 300°C, which is a practical level of energy conversion devices for any solid-state electrolyte at an intermediate temperature.[43,44]

The solid materials have a liquid-like ion conductivity, possibly because of the confinement of molecular mobility of ionic liquids in the nanosized spaces of the interfaces of the particles of silica. A nanoscale effect on the conducting properties was observed. The volume fraction of the ionic liquid in the hybrid material can be increased up to 90 wt % when nanosized silica of particle size 7 nm (surface area 390 m^2 g^{-1}) is used; moreover, a significant enhancement in the power factor of Archie's law was clearly observed as the size of the silica particles was reduced to the nanoscale. This value increased to almost twice that observed in bulk liquids. These results indicate the possible existence of a

(41) A. J. Bhattacharyya, Maier, J. *Adv. Mater.* **2004**, *16*, 811.
(42) Maier, J. *Nat. Mater.* **2005**, *4*, 805.
(43) Neouze, M.-A.; Le Bideau, J.; Vioux, A. *Prog. Solid State Chem.* **2005**, *33*, 217.
(44) Neouze, M.-A.; Le Bideau, J.; Gaveau, P.; Bellayer S.; Vioux, A. *Chem. Mater.* **2006**, *18*, 3931.

nanosized effect on the transport properties of the ionic liquid at the inorganic interfaces. On the other hand, the confinement of the liquid molecules of the ionic liquid among the nanospaces of the inorganic silica particles results in the formation of the stable solid-state electrolyte at up to 300°C, even though they contain a large portion of liquid molecules. The interaction at nanoscale interfaces between liquids and solids may be responsible for the structural stability of the hybrid electrolyte materials without releasing the liquid conducting molecules; those are strongly confined in between the silica particles.

The hybrid electrolyte presented in this work can be regarded as a recently emerging class of solid-state conducting materials with a liquidlike ionic mobility over a wide range of temperatures.[45] From the point of view of applications, the materials might be potentially applied to industrial electrochemical devices, such as fuel cells or as membranes for water electrolysis and separation, with wide operating temperature and electrical potential ranges.

Supporting Information Available: Figures S1−S5 (PDF). This material is available free of charge via the Internet at http://pubs.acs.org.

CM0707814

(45) Mehnert, C. P.; Mozeleski E. J.; Cook, R. A. *Chem. Commun.* **2002**, 3010